An Observer-based MPC Approach by Sensing Primary Signals in Transformer-isolated Converters

Ya Zhang, Marcel A. M. Hendrix and Jorge L. Duarte
Eindhoven University of Technology
Department of Electrical Engineering
P.O. Box 513, 5600MB Eindhoven, The Netherlands
ya.zhang@tue.nl

***Abstract*—A digital control method combining primary-side sensing, observer and model-predictive-control techniques is proposed. A conventional isolated Flyback converter is chosen for demonstrating the method. The only measured signal is the drain-source voltage over the switch. Following a procedure of signal processing, state estimation and constraint problem formulation, the controller determines the optimal duty cycle ratio. The advantages of the proposed method include minimal overshoot and fast stabilization, converter state restriction, and measurement network simplification.**

Keywords*— *Flyback, observer, primary side sensing, model preditive control, model mismatch

I. Introduction

Because model-predictive-control (MPC) deals with constraints and optimizes stabilization trajectories, it is gaining increasing attention in power electronics as an alternative to traditional analog control [1]. An observer is adopted for state estimation when a plant faces difficulties or complexities in state measurements. It measures a part of the plant state variables and accordingly estimates the plant state [2]. The primary-side-sensing (PSS) technique requires no opto-coupler-based circuits and is commonly used in isolated power electronics [3], [4].

The work in this paper continues the research in [5], [6] and experimentally demonstrates the control method measuring the primary voltage in a Flyback converter. It measures the switch drain-source voltage, and by means of signal processing the output capacitor voltage is calculated. From that, an observer module estimates the state of the magnetizing inductor. Knowing the state of the converter, the model-predictive-control scheme can be applied.

The paper demonstrates the importance of taking into account measurement errors and model-mismatch while designing an observer. The state estimation is given based on a derived plant model. Mismatch between the model and how the actual plant behaves, influences the estimation accuracy. In addition to this, measurement error is inevitable in experiments and it adds up to the estimation error.

II. Flyback converter and the control diagram

A. Flyback Converter Model Derivation

It is assumed that the Flyback converter is ideal (no parasitic components) and lossless, as it is shown in Fig.1. The converter is therefore represented by three differential equations

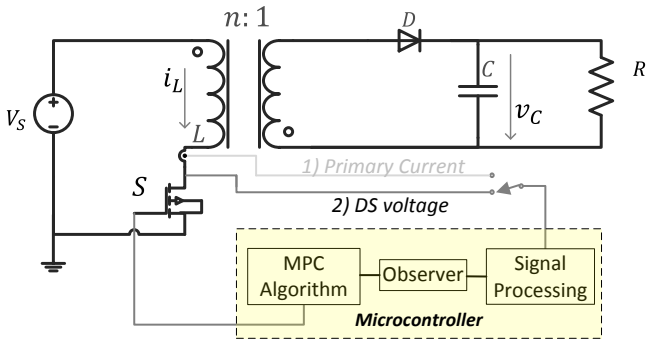

Fig. 1: System diagram

given in Table II, where i_L, v_C and D_t are the inductor current, capacitor voltage and duty cycle ratio value, respectively.

TABLE I: Flyback converter parameters

Definition	Symbol	Value	Unit
Magnetizing inductance	L	1.4	mH
Output capacitance	C	10	μF
Source voltage	V_s	100	V
Transformer transfer ratio	n	3	
Switching frequency	T_{sw}	10	μs
Load resistance	R	100	Ω

The converter parameters are summarized in Table I. It is presumed that the Flyback converter operates around a duty cycle ratio of $u_e = 0.6$ and it will result in a corresponding converter state given by $x_e = \begin{bmatrix}0.2083A & 25.00V\end{bmatrix}^T$, in continuous conduction mode (CCM). The first and second elements denote the averaged inductor current and the averaged capacitor voltage, respectively. They form the converter equilibrium point quantities:

$$\begin{aligned} u_e &= 0.6, \\ x_e &= \begin{bmatrix}0.2083A & 25.00V\end{bmatrix}^T. \end{aligned} \tag{1}$$

Following a process of state space averaging, model linearisation and discretization illustrated in [6], we can get a

TABLE II: State space representation of the Flyback converter, switched model.

SS description	$\dot{x_t} = Ax_t + b_t$ $x_t = \begin{bmatrix} i_L \\ v_C \end{bmatrix}$,	Dwell time
Switch ON, diode OFF	$A = A_1, b_t = b_{t,1}$ $A_1 = \begin{bmatrix} 0 & 0 \\ 0 & \frac{-1}{RC} \end{bmatrix}$ $b_{t,1} = \begin{bmatrix} \frac{V_s}{L} \\ 0 \end{bmatrix}$	$D_t T_{sw}$
Switch OFF, diode ON	$A = A_2, b_t = b_{t,2}$ $A_2 = \begin{bmatrix} 0 & \frac{-n}{L} \\ \frac{n}{C} & \frac{-1}{RC} \end{bmatrix}$ $b_{t,2} = \begin{bmatrix} 0 \\ 0 \end{bmatrix}$	$D_{t,1} T_{sw}$
Switch OFF, diode OFF	$A = A_3, b_t = b_{t,3}$ $A_3 = \begin{bmatrix} 0 & 0 \\ 0 & \frac{-1}{RC} \end{bmatrix}$ $b_{t,3} = \begin{bmatrix} 0 \\ 0 \end{bmatrix}$	$D_{t,2} T_{sw}$

simplified model of the converter, given by

$$\begin{aligned} x_{k+1} =& A_d x_k + B_d u_k, \\ y_k =& C_m x_k, \end{aligned} \tag{2}$$

where C_m is the measurement matrix, y_k the measured value, and A_d, B_d are constant matrices represented by the Flyback converter parameters and the equilibrium point quantities, and x_k and u_k are discrete small signals given by

$$\begin{aligned} u_k =& D_t - u_e \\ x_k =& x_t - x_e. \end{aligned} \tag{3}$$

Because the capacitor voltage is the only measured variable fed into the micro-controller, as highlighted in Fig.1, the inductor current (associated with the first element of x_k) has no contribution to the measured value y_k. The measurement matrix is therefore given by

$$C_m = \begin{bmatrix} 0 & 1 \end{bmatrix}. \tag{4}$$

B. Observer-Based Model Predictive Controller

1) Capacitor Voltage Calculation from DS Voltage : When the switch is OFF and the diode is ON, the switch drain-source voltage is

$$v_{DS} = V_s + n v_C, \tag{5}$$

where V_s is the source voltage and n the transformer primary-to-secondary transfer ratio. Accordingly the capacitor voltage is calculated.

2) Converter State Estimation by Observer: Now that the capacitor voltage is known, we are able to estimate the converter state accordingly. The observer elaborated on in [2] is adopted, described by

$$\hat{x}_{k+1} = A_d \hat{x}_k + B_d u_k + L_m (y_k - C_m \hat{x}_k), \tag{6}$$

where $\hat{x}_k$ is the estimation of x_k, and L_m is the observer feedback gain. Comparing (2) and (6) yields

$$x_{k+1} - \hat{x}_{k+1} = (A_d - L_m C_m)(x_k - \hat{x}_k). \tag{7}$$

Therefore, the observation design turns out to be a classic pole-placement problem, and that is, to place the eigenvalues of $(A_d - L_m C_m)$ within the unit cycle in the complex plane. The tunable parameter is L_m and A_d and C_m are constant matrices.

3) MPC for Trajectory Restriction: The algorithm is designed to fast stabilize the converter while considering the converter constraints and input efforts. Its mathematical description is to minimize the cost function defined by

$$\begin{aligned} F(x_0, U) =& x_N^T P x_N + \sum_{i=0}^{N-1} (x_i^T Q x_i + u_i^T R u_i), \\ \text{with } U =& \begin{bmatrix} u_0 & u_1 & \cdots & u_{N-1} \end{bmatrix}^T, \\ x_i =& A_d x_{i-1} + B_d u_{i-1}, \ i = 1, 2, \cdots N, \end{aligned} \tag{8}$$

where u_{i-1}, x_i are subjected to

$$\begin{aligned} u_{low,i} \leq& u_{i-1} + u_e \leq u_{high,i}, \\ \text{and } x_{low,i} \leq& x_i + x_e \leq x_{high,i}, \end{aligned} \tag{9}$$

and N is the prediction horizon; $u_{low,i,i=1\cdots N}$ and $u_{high,i,i=1\cdots N}$ are constraints about the input (associated with the duty cycle ratio); $x_{low,i,i=1\cdots N}$ and $x_{high,i,i=1\cdots N}$ are constraints about the state (associated with the inductor current and the capacitor voltage); P, Q, R are the weights on terminal state, the rest state, and the input, respectively [7].

III. Impacts of Measurement Error and Model Mismatch on Observation

The work in [5] demonstrates that the observer convergence time selection influences its performance. This section elaborates on additional criteria to assess an observer's performance: its abilities to deal with inevitable model mismatch and measurement errors.

A. Measurement Error

The analysis of measurement error is performed in absence of model mismatch. The normalized measurement offset error is defined as

$$\delta_y = \frac{\Delta y_\infty}{x_e(2)}, \tag{10}$$

where Δy_∞ is the static measurement error of the capacitor voltage, and $x_e(2)$ denotes the second element of x_e (the capacitor voltage at the equilibrium point). According to the analysis in section II-A, $x_e(2)$ can be also written as

$x_e(2) = C_m x_e$. The normalized observation offset error is defined as

$$\delta_{\hat{x}} = \begin{bmatrix} \frac{1}{x_e(1)} & 0 \\ 0 & \frac{1}{x_e(2)} \end{bmatrix} \Delta\hat{x}_\infty,$$

with

$$\Delta\hat{x}_\infty = \begin{bmatrix} \Delta\hat{x}_\infty(1) & \Delta\hat{x}_\infty(2) \end{bmatrix}^T \tag{11}$$

where $\Delta\hat{x}_\infty$ is the state estimation error when the observer is in steady state. The observation error gain from the measurement error is defined as

$$G_{mag} = \frac{\delta_{\hat{x}}}{\delta_y}. \tag{12}$$

Next, we show a procedure to derive the algebraic expression of the observation error gain. When the observer is in steady state, equations

$$\begin{aligned} \hat{x}_{k+1} &= \hat{x}_\infty \\ \hat{x}_k &= \hat{x}_\infty \\ y_k &= y_\infty, k \to \infty \end{aligned} \tag{13}$$

hold for (6). When there is no measurement error, y_k and $\hat{x}_k$ are zero. Therefore, the offset errors are $\Delta y_\infty = y_\infty - 0$ and $\Delta\hat{x}_\infty = \hat{x}_\infty - 0$. Substituting $\hat{x}_{k+1} = \hat{x}_k = \hat{x}_\infty = \Delta\hat{x}_\infty$ and $y_k = y_\infty = \Delta y_\infty$ into (6), and by comparing (11) and (10) , we get the explicit algebraic expression of the error gain

$$G_{mag} = \begin{bmatrix} \frac{1}{x_e(1)} & 0 \\ 0 & \frac{1}{x_e(2)} \end{bmatrix} (I - A_d + L_m C_m)^{-1} L_m C_m x_e. \tag{14}$$

This gain is independent of the measurement offset error Δy_∞ and dependent on the chosen equilibrium point.

B. Observer Design by Pole Placement

The function of an observer is to estimate a system state in a certain time interval. The observer design by pole placement is simple and effective for linear models, as it is illustrated in [2]. Bessel Polynomials further simplify the observer design by indicating the pole locations. However, practical systems have imperfect models and are therefore sensitive to model derivation errors and measurement inaccuracies. Consequently, the effectiveness of observer design by pole placement can be compromised.

1) Closed Loop Observer Design by Pole Placement: the observer settling time $650\mu s$ is borrowed from [6] which demonstrated an effective current observer with the same observer settling time. Bessel polynomials are adopted for pole placement. The resulting observer gain matrix and its corresponding error gain factor are

$$\begin{aligned} L_{m,1} &= \begin{bmatrix} -0.1056 & 1.1494 \end{bmatrix}^T, \\ G_{mag,1} &= \begin{bmatrix} -39.5568 & 0.1876 \end{bmatrix}^T \end{aligned} \tag{15}$$

respectively. The error gain indicates that -1% offset error in measuring the voltage will lead to an estimation offset error of 39.5% in current, -0.187% in voltage, as highlighted by the blue small solid sphere in Fig.2.

Since the estimation error is linearly proportional to the measurement error, the observer becomes more inaccurate when the measurement error increases (see Fig.2 for the example of -5% measurement error). Please note that the observation error gain discussed here is oriented to the chosen equilibrium point given in (1).

2) Open Loop observer: An open loop observer (not feasible in practice) is obtained by setting the observer gain $L_{m,0} = \begin{bmatrix} 0 & 0 \end{bmatrix}^T$. It means the observer disregards the information from the measurement, and there is no communication between the converter and the controller. Consequently, the measurement error has no influence on the estimation and from (12) we have $G_{mag,0} = 0$.

C. Observer Design Adaptation

An observer designed by pole placement is confined to coordinate the convergence speed. The tolerance to measurement and model derivation errors is not regarded or promised by this method. The observer obtained by the method of pole placement in section III-B1 is very sensitive to the measurement error. A open loop observer discards converter measurement information and makes itself very dependent on the correctness of the derived converter model. Hence, the observer is heuristically adjusted towards a small error gain G_{mag} (not a zero gain). The extreme design is to set the observer gain matrix $L = \begin{bmatrix} 0 & 0 \end{bmatrix}^T$ (resulting in a zero error gain). It is not feasible in practice, but it indicates that an observer gain matrix whose elements are close to zero could be a solution. Please note that a small observer gain matrix (not zero) will prolong the observer convergence time from (7). This means that the MPC algorithm cannot give reasonable response in time and overshoots are possible.

An observer with a relatively small error gain is found after a series of manual attempts. The resulting observer gain matrix and its corresponding error gain factor are

$$\begin{aligned} L_{m,2} &= \begin{bmatrix} -0.0106 & -0.0460 \end{bmatrix}^T, \\ G_{mag,2} &= \begin{bmatrix} 1.0698 & -0.0612 \end{bmatrix}^T, \end{aligned} \tag{16}$$

respectively. The observer with the adapted observer gain matrix is chosen because it yields a relatively small error gain. As a consequence, the observer becomes more tolerant to the measurement error compared to the one obtained by pole-placement. Despite the fact that this observer results in $122\mathrm{ms}$ observation settling time, it is adopted for the experiments and we have $L_m = L_{m,2}$.

D. Model Mismatch

1) Switched Model and Simplified Model: The premise for an observer design is an accurate model of the converter. Regardless of power loss and parasitic components, the most accurate model for the Flyback converter is the switched model

described in Table II. However, adopting this switched model makes an observer design very complex. A common solution is model simplification by means of averaging and linearisation.

As a consequence, the simplified linear model is not equal to the original switched model. According to the parameters in Table I, the pairs of the converter steady state (inductor current and capacitor voltage) and a given duty cycle ratio with these two different models are plotted in Fig.2: *Switched model* refers to the one described in Table II; *Simplified model* denotes the one in (2) given by $(x_\infty + x_e)$. Please note that the *Switched model* takes into account both continuous and discontinuous conduction modes, while the *simplified model* is the small signal model linearised at $D_t = 0.6$.

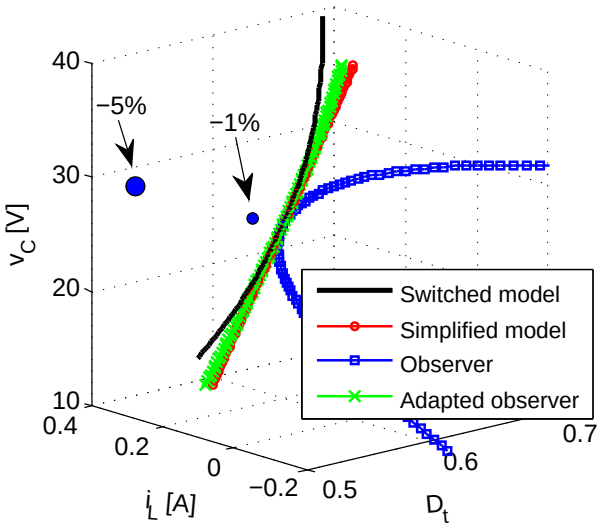

Fig. 2: Visualization of model mismatch and observation error

2) Model-Based Observation: The pairs of the converter steady state (inductor current and capacitor voltage) and a given duty cycle ratio with different observers are plotted in Fig.2: *Observer* indicates the estimated converter state $(\hat{x}_\infty + x_e)$ with $L_m = L_{m,1}$ and *Adapted observer* refers to the state with $L_m = L_{m,2}$. Both observers give estimation based on equation (6).

IV. Experimental Results

A. Set-up Description and Implementation

Fig.3 shows the Flyback converter system. The type of the DSPACE is *DS1104 R&D Controller Board* associated with software *Control Desk 5.1*. The oscilloscope is *HDO 4024, 200MHz high definition oscilloscope 2.5Gs/s.* The parameters for the MPC algorithm are summarized in Table III.

B. Results and Discussion

Fig.4 and Fig.5 display the experimental results captured by the digital controller and by the oscilloscope, respectively. The converter initial state is set by feeding a constant duty cycle ratio value to the plant (in open loop). The reference is set in advance by the digital controller. At a certain moment,

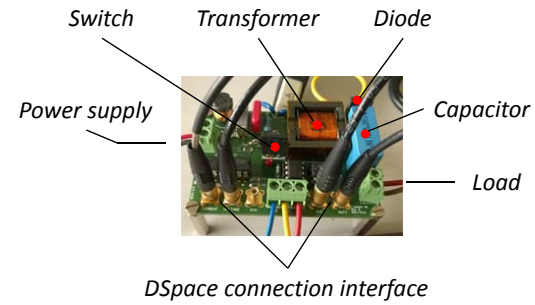

(a)

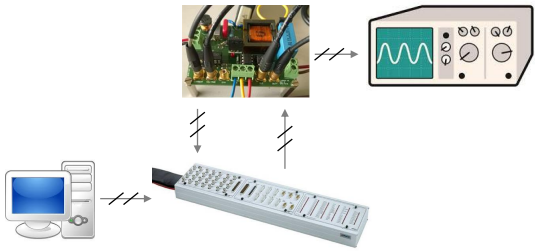

(b)

Fig. 3: Experimental set-up description: (a) Flyback converter board; (b) system connection diagram.

TABLE III: Controller parameters

parameter	value
weight on i_L	$\frac{1}{x_e(1)}$
weight on v_C	$\frac{100}{x_e(2)}$
weight on u	$\frac{1}{u_e}$
$u_{low,i=0\ \ldots N-1}$	0.1
$u_{high,i=0\ \ldots N-1}$	0.7
$x_{low,i=0\ \ldots N-1}$	$\begin{bmatrix}0 & 0\end{bmatrix}^T$
$x_{high,i=0\ \ldots N-1}$	$\begin{bmatrix}0.6\text{A} & 34\text{V}\end{bmatrix}^T$
sampling time T_s	330µs
prediction horizon	5
control horizon	1

a *button* is pressed to close the control loop and the controller becomes active.

As it is shown in Fig.4, the red arrow points out the instant when the controller is activated. The reference is plotted in bold solid black line; the blue solid line with discrete dots refers to the observed trajectory of the converter.

The top curve of Fig.5 shows the trace of the Flyback converter primary current which is detected by a current probe in series with transformer primary side. The middle one is the averaged primary current which is obtained by using a shunt resistor with an analog low-pass filter. The bottom one is the capacitor voltage measured by a voltage probe placed in parallel with the load.

It can be seen in both figures that the converter state approaches the pre-set reference and the convergence trajectory stays in its pre-set margins. No objectionable overshoot is

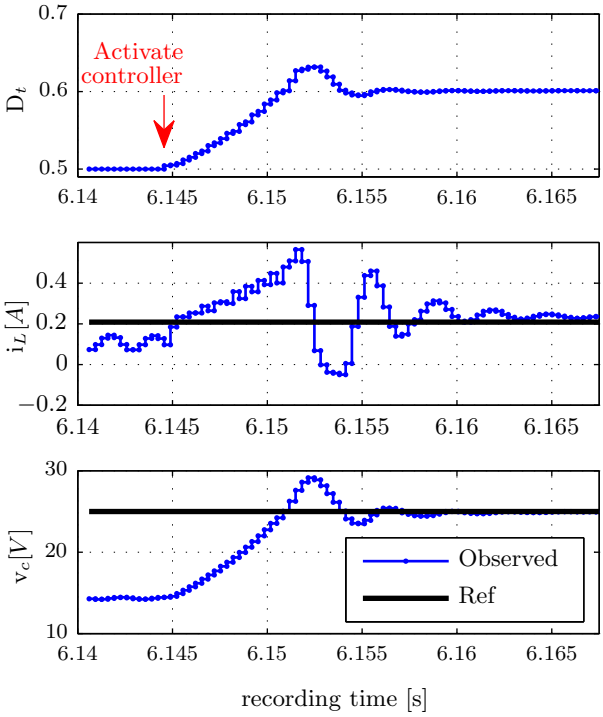

Fig. 4: Experimental results when using the adapted observer, captured by the digital controller. From the top to the bottom are duty cycle ratio, averaged inductor current and capacitor voltage.

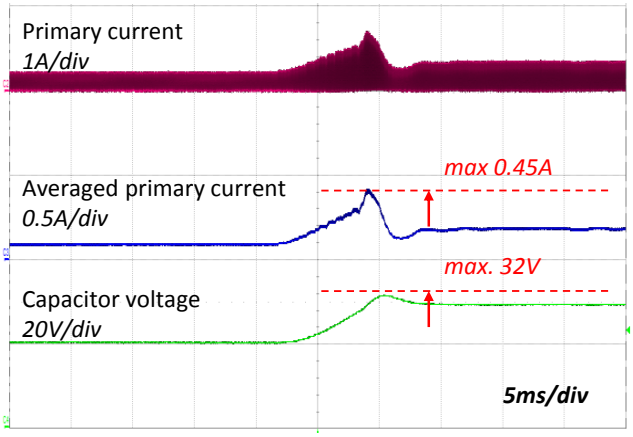

Fig. 5: Experimental results when using the adapted observer, captured by the oscilloscope. From the top to the bottom are primary current through the switch, averaged primary current and capacitor voltage.

visible. Because the measurement takes place on the converter primary side, no sophisticated feedback network is needed.

V. Conclusion and Recommendations

The aim is to design an observer which is both fast and tolerant to measurement error and model mismatch. A simple pole-placement method is not sufficient to design a decent observer because it only takes into account observation speed and disregards the existence of modelling error and measurement error. It is essential to check the observer error gain before experiments. This paper demonstrates an effective voltage observer measuring the switch drain-source voltage in the Flyback converter.

It is recommended to use an observer which can compensate the mismatch between original and simplified models, at least not to enlarge the difference. Due to the existence of measurement errors, it is necessary to check the observer's tolerance to the measurement errors before applying it in practice.

References

[1] V. Spinu, A. Oliveri, M. Lazar, and M. Storace, "Fpga implementation of optimal and approximate model predictive control for a buck-boost dc-dc converter," in *Control Applications (CCA), 2012 IEEE International Conference on*, Oct 2012, pp. 1417–1423.

[2] R. J. Vaccaro, *Digital control: a state-space approach*. McGraw-Hill New York, 1995, vol. 196.

[3] C.-W. Chang, Y.-T. Lin, and Y.-Y. Tzou, "Digital primary-side sensing control for flyback converters," in *Power Electronics and Drive Systems, 2009. PEDS 2009. International Conference on*, Nov 2009, pp. 689–694.

[4] X. Xie, J. Wang, C. Zhao, Q. Lu, and S. Liu, "A novel output current estimation and regulation circuit for primary side controlled high power factor single-stage flyback led driver," *Power Electronics, IEEE Transactions on*, vol. 27, no. 11, pp. 4602–4612, Nov 2012.

[5] Y. Zhang, M. A. M. Hendrix, and J. L. Duarte, "Ccm flyback converter using an observer-based digital controller," in *2015 IEEE International Conference on Industrial Technology*, March 2015, pp. 2056–2061.

[6] Y. Zhang, M. A. M. Hendrix, J. L. Duarte, and E. A. Lomonova, "Flyback converter using an observer-based digital controller," in *17th European Conference on Power Electronics and Applications*, August 2015.

[7] V. Spinu, J. Schellekens, M. Lazar, and M. Hendrix, "On real-time optimal control of high-precision switching amplifiers," in *System Theory, Control and Computing (ICSTCC), 2013 17th International Conference*, Oct 2013, pp. 507–515.